Lethal by design? Guiding environmental assessments of ocean alkalinity enhancement toward realistic contextualization of the alkalinity perturbation

Lennart T. Bach[1*], Michael D. Tyka[2], Bin Wang[3], Katja Fennel[3]

[1]Institute for Marine and Antarctic Studies, University of Tasmania, Hobart, Tasmania, Australia

[2]Google Inc., Seattle, Washington, USA

[3]Department of Oceanography, Dalhousie University, Halifax, Nova Scotia, Canada

*Corresponding author: lennart.bach@utas.edu.au

Abstract

Ocean Alkalinity Enhancement (OAE) aims to mitigate climate change by increasing the chemical capacity of seawater to store anthropogenic CO_2. OAE can be implemented through multiple pathways, each of which intentionally modifies marine carbonate chemistry through increases in total alkalinity (TA). Experimental research has only recently begun to assess how such TA perturbations (ΔTA) affect ocean geochemical processes and ecosystems. Meaningful assessments need context on how ΔTA induced by different OAE pathways would evolve over time and in magnitude. Here, we use a dilution equation, a regional model, and a global model to explore how marine systems and life styles would experience ΔTA under realistic constraints. We find that a more extreme ΔTA of >1000 µmol kg^{-1}, a perturbation commonly considered in OAE experiments, only occurs for minutes in a miniscule fraction of the OAE-perturbed seawater volume. In contrast, ΔTA between 1-100 µmol kg^{-1} is a ubiquitous perturbation range for OAE under real-world constraints, yet rarely in focus of environmental OAE assessments. These results suggest that there is a disconnect between real-world ΔTA that can plausibly be invoked by OAE and the

29 experimental ΔTA range frequently used in the context of the environmental OAE
30 assessment. While “unrealistic” ΔTA can provide crucial insights into response patterns to
31 OAE, they can also cause overestimation of OAE effects, if the unrealistic ΔTA is not
32 contextualized appropriately. Our results can be used to improve the contextualization of
33 OAE studies, thereby making the interpretation of ΔTA effects on the environment more
34 robust.
35
36 **1. Introduction**
37
38 Ocean Alkalinity Enhancement (OAE) encompasses marine CO_2 removal (mCDR) pathways
39 that increase sea surface alkalinity and thus the storage of atmospheric CO_2 in seawater
40 (Renforth and Henderson 2017, Eisaman *et al* 2023). OAE is inspired by chemical reactions
41 that occur during natural rock weathering. When alkaline minerals are exposed to water, their
42 slow dissolution converts CO_2 dissolved in water into dissolved bicarbonate (HCO_3^-), thereby
43 enabling additional atmospheric CO_2 absorption by the liquid. This weathering reaction
44 contributes to balancing atmospheric CO_2 over hundred thousand year timescales (Archer *et*
45 *al* 2009, Penman *et al* 2020). OAE aims to accelerate weathering to sequester CO_2 much
46 faster than this natural process could without human intervention.
47
48 OAE can be implemented through diverse pathways that differ in the source and treatment of
49 alkaline material, the alkalising agent used to deliver alkalinity to the ocean, and the
50 environment in which it is applied. For example, some pathways source alkaline rock, grind
51 it, and distribute it on seafloor sediments where they dissolve over years (Geerts *et al* 2025).
52 Other pathways employ different types of electrochemical treatment to remove hydrochloric
53 acid from seawater and leave hydroxide-enriched (instantaneously more alkaline) seawater
54 behind (Eisaman *et al* 2023). All OAE pathways are associated with pathway-specific
55 “collateral” (unintentional) perturbations that need to be assessed on an individual basis. In
56 the examples above, dissolution of alkaline rock would unintentionally enrich seawater with

57 rock-specific trace metals (Hartmann *et al* 2013), whereas the instantaneous alkalinity
58 increase through electrochemistry would cause relatively strong transient pH excursions
59 (Ferderer *et al* 2022). However, common to all OAE pathways is the intentional increase in
60 seawater (bi)carbonate concentration, measurable as an increase in total alkalinity (TA).
61
62 The continuous emissions of CO_2 into the atmosphere and the increasing dependence on
63 gigatonne-scale CDR to keep global warming below 2°C has promoted interest in CDR
64 (Smith *et al* 2024), including OAE (Oschlies *et al* 2023). To assess the feasibility of OAE it is
65 essential to evaluate its environmental effects before considering any potential
66 implementation at larger scales (Bach *et al* 2019). This assessment has already commenced
67 and is dependent on experimental studies that simulate TA perturbations (ΔTA) to determine
68 corresponding responses of biological and geochemical processes (Dupont and Metian
69 2023, Iglesias-Rodríguez *et al* 2023). However, an emerging inconsistency among OAE
70 experiments is the level of ΔTA that is tested and compared to experimental controls. These
71 range from 10^1 - 10^6 µmol kg^{-1} in short-term experiments (<2 days) to 10^1 - 10^3 in longer-term
72 experiments (>2 days). The question these large gradients raise is to what extent a tested
73 level ΔTA represents a perturbation in the ocean under real world constraints. When outside
74 the range representative for OAE, an experiment could under- or overestimate the
75 environmental effects of ΔTA as it can be expected that the effects scale with the magnitude
76 of ΔTA. Indeed, similar concerns about the implications of non-representative perturbation
77 ranges to study the effects of an environmental driver have been expressed during the early
78 days of other emerging research fields, for example ocean acidification research (Barry *et al*
79 2010).
80
81 Here, we aim to inform the environmental OAE assessment by exploring ΔTA that could be
82 caused by OAE under real-world constraints. To achieve this, we determine how TA would
83 technically be delivered to the ocean under OAE and which first-order constraints limit its
84 delivery. Thereafter, we use a dilution model, a regional model, and a global model to

simulate ∆TA within these realistic margins and determine how the environment experiences ∆TA over space and time. Results are compared to ∆TA studied in previous OAE experiments. Importantly, our study focuses on ΔTA, the intentional change common to all described OAE pathways. We do not address collateral perturbations (e.g., trace metal additions), which are unintentional side effects and highly specific to individual OAE pathways.

2. Constraints on alkalinity perturbations

2.1. Drivers of alkalinity perturbations

The diverse range of OAE pathways and their corresponding alkalising agents differ widely (Eisaman *et al* 2023). However, with regard to their effect on seawater TA, all pathways can be broadly categorized into fast- and slow-dissolving alkalising agents (Dupont and Metian 2023). Fast-dissolving agents such as acid-depleted brine (House *et al* 2007) or calcium hydroxides (Kheshgi 1995) dissolve within seconds to hours and therefore rapidly elevate TA at their deployment site (Caserini *et al* 2021, Savoie *et al* 2025). These agents can be added from point sources or ships where the acute ∆TA is highly localized (Fig. 1). In contrast, slow-dissolving agents such as forsterite (Geerts *et al* 2025) or calcium carbonate sand (Fuhr *et al* 2025) release TA over weeks to years. These agents are distributed over much larger areas of sediment, where they slowly dissolve and cause a small (per kg of seawater) but spatially more distributed and chronic ∆TA (Fig. 1).

Numerical modelling suggests that ∆TA declines with distance from the TA addition site due to mixing and dilution (He and Tyka 2023, Mu *et al* 2023, Wang *et al* 2023, Khangaonkar *et al* 2024, Zhou *et al* 2025, Wang *et al* 2025). As such, the spatio-temporal evolution of ∆TA depends on (1) the physical processes that determine ocean mixing, (2) the amount of TA added at a given location per time, and (3) the characteristics of the alkalising agent. Physical mixing in the ocean differs profoundly both spatially and in time (Moum 2021) and

OAE operations would have to adapt to local conditions to control the environmental exposure. This could be achieved by adjusting the amount of added alkalising agents and its characteristics (e.g. dissolution and sinking rate (Wang *et al* 2025)). Decisions on the amounts and characteristics to be added would depend on a number of factors (NASEM 2022), including scalability potential, limits set by (local) policies, and local physical and geochemical constraints (Wang *et al* 2025). These factors set boundaries on ΔTA under real world constraints that will inform the modelling undertaken herein.

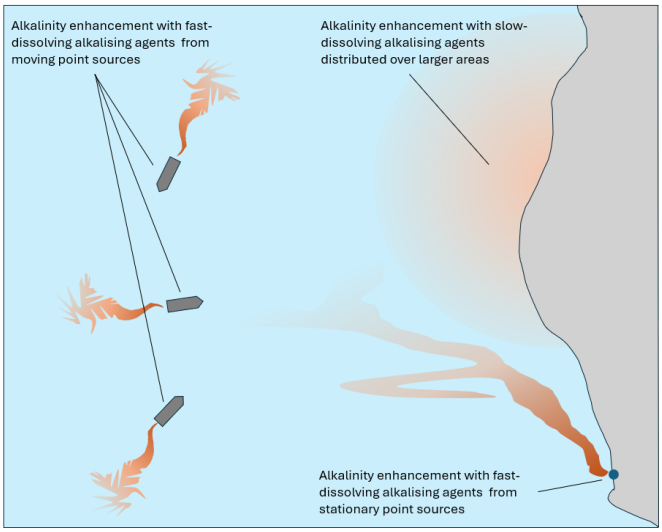

Figure 1. Alkalinity enhancement in the environment. Fast-dissolving alkalising agents (e.g. NaOH, $Ca(OH)_2$, or hydrated carbonates) dissolve immediately causing initially high and highly localized ΔTA, which spreads out and declines as it dilutes over time. Slow-dissolving alkalising agents (e.g. forsterite sand) distributed over larger areas dissolve over many years, causing low, constantly replenished ΔTA.

2.2. Scalability constraints on alkalinity perturbations

Each of the many OAE pathways is associated with specific logistical or technological constraints (Eisaman *et al* 2023). For example, while the availability of alkaline rock may not limit the upscaling of mineral-based OAE (Caserini *et al* 2022), the treatment and distribution

of that rock likely would (Caserini *et al* 2021). Similarly, for electrochemical methods, even if renewable energy is not a limiting factor, the generation of strong acid by-products requiring disposal could constrain their scalability (Eisaman 2024). Since solutions for these and other factors are difficult to predict, it may be more useful to follow (Renforth and Henderson 2017) and ask more broadly how other industries that move gigatonnes of mass have grown in the past. Renforth and Henderson's (2017) example was the global cement industry, which extracts ~7 Gt of material per year. Assuming an extremely optimistic growth rate of 25% (current solar electricity growth (Graham *et al* 2025)) OAE would take around 30-40 years to scale to 7 Gt CO_2 y^{-1} (Renforth and Henderson, 2017). Estimates of CDR required in 1.5–2°C scenarios in 2050 range between 6–10 Gt CO_2 y^{-1}, achieved through a portfolio of CDR methods with OAE potentially being one of them (Gidden *et al* 2024). Based on these boundaries, we make the very optimistic assumption that OAE might scale to ~10 Gt CO_2 y^{-1}, which, even under ideal circumstances, would take decades to be achieved. As such, our global model (section 3.2.3.) simulates induced CDR through OAE of around 10 Gt CO_2 y^{-1}.

2.3. Regulatory constraints on alkalinity perturbations

To the best of our knowledge, there is currently no specific governance to regulate OAE. The London Convention (LC, currently 87 member states) prohibits dumping specifically listed materials while the London Protocol (LP, currently 53 member states) allows dumping of specifically listed materials. Amendment LP.4(8) to the LP (currently ratified by 6 LP member states) prohibits "marine geoengineering" except for legitimate scientific research. The amendment only lists ocean fertilization but there have been recent considerations to also include OAE and other marine CDR approaches (IMO 2023). LP.4(8) is not legally binding as this requires two thirds of LP member states to ratify it. Thus, it has currently only normative weight (Brent *et al* 2018). However, even if it became legally binding, LP.4(8) would simply prohibit OAE and not provide guidance on what degree of perturbation is permissible. It may therefore be more meaningful to explore existing regulation that is relevant for TA discharge

outside the OAE context. For example, wastewater treatment uses TA (sodium hydroxide (NaOH) or calcium hydroxides) to keep wastewater pH within regulatory limits before the wastewater is discharged (Tchobanoglous *et al* 2013). We explored repositories by the Food and Agriculture Organization and other data sources to find that upper pH limits for dischargeable wastewater vary across countries (or even states within countries) between 8.5 and 9.5 (Table S1).

To inform our dilution and regional modelling, we assume that regulation for OAE perturbation limits (i.e. the upper pH limit) will follow the precedent set by wastewater discharge regulation. We therefore adopt pH_T 9 (total pH scale) as the upper limit the pH can have within a mixing zone when the TA that is added from a point source in a grid field of the model causes a pH increase. pH_T 9 (and not 8.5 or 9.5) was chosen as it is the middle value and also the relevant threshold in Halifax Harbour where regional model simulations were performed (section 3.2.2.).

2.4. Geochemical constraints on alkalinity perturbations

Secondary carbonate precipitation (e.g. $CaCO_3$ or $MgCO_3$) sets a geochemical constraint on OAE efficiency by consuming TA after its delivery (Fuhr *et al* 2022, Moras *et al* 2022, Hartmann *et al* 2023). OAE increases the risk for carbonate precipitation as it elevates the carbonate saturation states defined as:

$$\Omega = \frac{[Ca^{2+}]_{SW} \times [CO_3^{2-}]_{SW}}{K_{Sp}} \quad (1)$$

where Ca^{2+} and CO_3^{2-} are the concentrations of these ions in seawater and K_{Sp} is the solubility product for $CaCO_3$. In the worst case, OAE-induced oversaturation can trigger so-

187 called “runaway precipitation” leading to TA loss larger than what was initially delivered via
188 OAE (Fuhr *et al* 2022, Moras *et al* 2022, Hartmann *et al* 2023).
189
190 Inorganic particles play an important role for TA loss as they can function as “seeds” to
191 catalyse carbonate precipitation (Morse *et al* 2007, Zhong and Mucci 1989). Pelagic
192 environments do generally not provide enough seeds for relevant precipitation to occur at
193 relevant rates, even under extreme levels of OAE. For example, precipitation was not
194 detectable in OAE experiments with plankton communities where TA was stable for 22-33
195 days at Ω_{Arg} ~3-10 for the $CaCO_3$ mineral aragonite (Paul *et al* 2024). Likewise, geochemical
196 OAE experiments found no TA loss for 25 days at Ω_{Arg} of ~13 (Suitner *et al* 2024), conditions
197 where pH was much beyond 9 and thus over the regulatory threshold we defined above. As
198 such, geochemical limits via secondary precipitation would likely be a lower-level constraint
199 in most pelagic environments relative to acceptable pH limits. Some notable exceptions to
200 this may occur in estuaries (Wurgaft *et al* 2021), surf zones (England and Bach 2025), or
201 shallow environments with resuspended carbonate particles (Morse *et al* 2007).
202
203 In contrast to most open water, secondary precipitation of carbonates and even clays is
204 potentially a major constraint to how much TA can be added to coastal seafloor sediments
205 (Geerts *et al* 2025). In pore waters, seeds are abundant but quantifications of TA loss therein
206 are limited and differ across sediment types, composition, and oxic state (Geerts *et al* 2025).
207 Deriving a threshold OAE intensity is therefore premature at this point, but we assume that
208 OAE-induced pH increases need to be much lower than in pelagic environments (i.e.,
209 pH<<9).
210
211 **3. Methods**
212
213 **3.1. Literature analysis of currently widespread alkalinity perturbation ranges**
214

A literature analysis was performed to provide an overview of the levels of ΔTA currently studied in OAE experiments. To gather relevant literature we conducted a Google Scholar search with the following search query: “Ocean Alkalinity Enhancement” OR “Ocean Alkalinization” OR “Ocean Alkalisation” (1.4.2025) and went through the first 200 hits, sorted by Google Scholar according to relevance. Furthermore, we worked through the reference lists of the marine CDR report by the National Academy of Science and Medicine (*NASEM*, 2022) and the OAE best practice guide (Oschlies *et al* 2023). Studies that were included in this analysis had to be (1) peer-reviewed, (2) consider OAE as within the context of their study, (3) reported TA (or TA could be calculated with reported data), and (4) not use forsterite or other slowly dissolving alkalising agents because in these cases ΔTA is constantly changing over the course of an experiment.

3.2. Model simulations

3.2.1. Alkalinity addition from a ship

Delivery of an alkalising agent offshore would likely depend primarily on ships (Caserini *et al* 2021, Gentile *et al* 2022, He and Tyka 2023). Offshore delivery requires that the alkalising agent dissolves quickly before sinking into deeper water masses where increased TA would not immediately enable uptake of atmospheric CO_2 (Köhler *et al* 2013). We calculated the dilution of ΔTA over time (t) following He and Tyka (2023) as:

$$\Delta TA(t) = \frac{1}{D(t)} \times C_0 + \left(1 - \frac{1}{D(t)}\right) \quad (2)$$

where C_0 is the effluent concentration of the alkalising agent (C_0 in mol/L). D was calculated following IMCO (1975):

$$D(t) = \frac{0.0045}{Q} \times U^{1.4} \times L^{1.6} \times t^{0.4} \quad (3)$$

and Chou (1996):

$$D(t) = \frac{0.2108}{Q} \times U^{1.552} \times B^{1.448} \times t^{0.552} \quad (3)$$

Here, Q is the release rate of alkalising agent (m^3/s), U is ship speed (m/s), L is the waterline length (m) or B is the beam width of the ship (m). ΔTA(t) was calculated for 3 common ship types that could be used for delivery: Suezmax (Q=1.2 m^3/s, U=7.7 m/s, L=375 m, B=55 m); Panamax (Q=0.7 m^3/s, U=6.7 m/s, L=270 m, B=35 m), 20k DWT (Q=0.25 m^3/s, U=5.1 m/s, L=175 m, B=20 m). All these vessels are simulated to release immediately dissolving TA with an effluent concentration of 1 mol/L.

3.2.2. Regional model

To illustrate typical exposures experienced by organisms at coastal sites, we use a high-resolution implementation of the Regional Ocean Modelling System (Haidvogel *et al* 2008) for Halifax Harbour (Canada) and map typical ranges in TA as a result of a point-source addition and the dissolution of feedstock on the seafloor. The model configuration uses three nested grids with increasing horizontal resolution (1 km in the outermost grid, 183 m for the next grid embedded within, and 61 m in the innermost grid) as described in Wang *et al* (2025). All three grids have 40 terrain-following vertical layers and are forced by atmospheric data from the ECMWF ERA5 reanalysis by Hersbach *et al* (2020). In addition, the sea surface temperature in the outermost domain is relaxed toward satellite observations from Donlon *et al* (2007). The initial and open boundary conditions for the outermost domain are derived from the data-assimilative GLORYS product by Jean-Michel *et al* (2021) with tidal forcing provided by Egbert and Erofeeva (2002).The three model domains can be run sequentially such that results from the coarser domain provide lateral boundary conditions for

the next-higher resolution model. Alternatively, the two inner domains can be run simultaneously in 2-way coupled mode where they continuously exchange information about in- and outflow across the shared lateral boundary. Freshwater input from land is only considered in the two higher-resolution models where freshwater input from the Sackville River is prescribed according to observations (Wateroffice Canada 2025) and other rivers are scaled to the Sackville River following Shan *et al* (2011). Freshwater input from sewage plants in Halifax is prescribed using a climatological estimate from the Mill Cove plant at the head of the harbour which we consider to be representative of the other sewage plants (Halifax Water 2025). An extensive validation of the model as well as estimates of water residence time in the harbour basin are presented in Wang *et al* (2025).

Multiple 3-month runs of the two-way nested model were performed for point source additions through coastal outfalls starting on the first of January, April, July, and October of 2020 for an outfall at the Tufts Cove power plant. Additional simulations, starting on July 1, were run for an outfall at the head of the Basin (Mill Cove) and outside the harbour in a small embayment near Ketch Harbour (see Fig. 3 for outfall locations). In order to choose an addition rate near the upper limit of what is allowable within the constraint of pH (total scale) < 9, we inspected the evolution of ΔTA in the grid cell receiving the TA addition (Fig. S1). The evolution of ΔTA is highly variable, suggesting that pH will have to be closely monitored for operational deployments, and dosing dynamically adjusted to current conditions. For the simulations presented in this analysis, we chose constant addition rates that result in temporary overshoots of the ΔTA threshold that corresponds to $pH_T = 9$. Allowing overshoots to occur between 12% to 14% of the time in the grid box of the TA addition, we settled on a constant addition rate of 12.5 mol/s for Tufts Cove (the tidally mixed channel), 3 mol/s at Mill Cove (at the head of Bedford Basin), and 0.8 mol/s at Ketch Harbour (a small embayment outside the harbour).

Furthermore, a 2.5-year simulation starting in January 2018 was performed with a homogenous TA addition at the seafloor across Bedford Basin mimicking slow dissolution of a feedstock evenly distributed across the seabed. The assumed addition rate in this case was 1 mol s^{-1}. Since the area of Bedford Basin is 17.5 km^2 this amounts to 0.057 mol km^{-2} s^{-1}). This simulation of OAE through mineral weathering on the seafloor assumes much lower rates of TA additions per area due to the higher risk of secondary precipitation at the presence of seed particles that could catalyze secondary precipitation (section 2.4.).

3.2.3. Global model

To inform the typical changes in TA which could be expected in a steady-state deployment of OAE on a global scale, we reanalyzed simulation data from He and Tyka (2023). The circulation model used in that study was the ECCO (Estimating the Circulation and Climate of the Ocean) LLC270 physical fields with a 1/3° degree horizontal resolution (Zhang *et al* 2018). The LLC270 configuration used a latitude-longitude-cap (LLC) horizontal grid with a horizontal resolution ranging from 7.3 km at high latitudes to 36.6 km at low latitudes. It comprised 50 vertical layers ranging from 10 m thick at the ocean surface to 458 m at the bottom (Zhang *et al* 2018). The iteration-42 state estimate described in Carroll *et al* (2020) was used as the starting point. The gchem and dic packages within MITgcm were used to represent the ocean carbonate system. The ocean carbon model was based on Dutkiewicz *et al* (2005) and used 5 biogeochemical tracers (DIC, TA, phosphate, dissolved organic phosphorus, and oxygen). The tracers were advected and mixed by the physical flow fields from the circulation model, and the sources and sinks of DIC were: CO_2 flux between the ocean and atmosphere, freshwater flux, biological production, and the formation of calcium carbonate shells. The wind speeds used to calculate the gas exchange were imported from the LLC270 forcing data and the air-sea exchange of CO_2 was parameterized with a uniform gas transfer coefficient (Wanninkhof 1992). The biogeochemical tracers were initialised with contemporary data from GLODAPv2 mapped climatologies (Lauvset *et al* 2016) where

possible, or using data from Dutkiewicz *et al* (2005) and were allowed to relax locally by running 100 years of forward simulation (looping the 1992-2017 ECCO forcing fields). For simplicity, atmospheric pCO_2 was held constant at 415 µatm, rather than trying to anticipate future emission scenarios. Since in the analysis of the present work we focus merely on the dispersion of TA, which is a conserved tracer in the model, this simplification should not affect the results.

Three OAE scenarios were analyzed: One, in which TA was released in strips along all coastlines (111 km thick) and two in which it was released in individual point locations spaced 200 or 400 km along the coast, respectively. In all simulations the local TA addition rate was adjusted such that the local change in pH_T, relative to an unperturbed background simulation, did not exceed 0.1 pH_T unit. The total amount of yearly negative emissions achieved in these scenarios was 9 $GtCO_2$ yr^{-1} for the continuous strip release and 11 $GtCO_2$ yr^{-1} and 8.2 $GtCO_2$ yr^{-1} for the point release scenarios (at 200 or 400 km site separation, respectively). Each simulation was run for 19 years.

We analyzed the ΔTA over the entire surface ocean, at steady state, which is reached after roughly 4 years. These simulations do not attempt to model the dispersion dynamics of point releases below a resolution of the model (7-35 km) but rather try to answer the question of what the steady state ΔTA would look like in the far field only.

4. Results

4.1. Alkalinity perturbations in environmental OAE experiments

The literature analysis returned 29 relevant OAE experiments (Table 1). The investigated ΔTA ranged roughly from 10 - 3400000 µmol kg^{-1} in experiments lasting between 0.007 days (10 minutes) to 55 days. Twentyone % of the experiments contextualized the simulated ΔTA

as a transient perturbation of a rapidly dissolving alkalising agent that is diluted with unperturbed seawater from the surrounding. Here, the initial ΔTA before the first dilution ranged between 100-3400000 μmol kg^{-1} and lasted between 10 minutes and 7 days. One experiment was a field study in a coral reef, where initial ΔTA was around 200 μmol kg^{-1} before the NaOH-perturbed seawater diluted across 25 m of tidal flow to reach 50.2 ± 2.7 μmol kg^{-1} in the central part of the plume (Albright *et al* 2016). The other 79% contextualized the experiment as scenarios where ΔTA is permanently elevated to a constant level and dilution does not occur. Here, ΔTA treatments ranged between 10-9200 μmol kg^{-1} and the experiments lasted for 2-68 days.

Table 1. *Results from the literature analysis on the magnitude and duration of ΔTA in environmental OAE experiments. Context "A" refers to experiments with a transient ΔTA diluted over time while "B" refers to experiments where ΔTA was constantly elevated. The inserted figure illustrates the ΔTA ranges explored in each study (grey lines with red (context A) and blue (context B) end points, but note that high endpoints are occasionally cut off due to the x-axis limit). For orientation we added: a distribution of ΔTA in the global surface ocean as shown in Fig. 4a; the ΔTA corresponding with pH 9 (free scale) as a regulatory constraint; ΔTA when rapid carbonate precipitation occurs as a geochemical constraint* (Suitner *et al* 2024).

Ecosystem/Organism or geochemical process	ΔTA (µmol kg^{-1})	Duration (days)	Context	Reference	Exp
Coral reef	50.2	0.04	A	Albright et al., 2016	1
Shore crab	180	0.25	A	Cripps et al., 2013	2
Oyster	41-322	24	B	Duckham, 2013	3
Phytoplankton	~340-3400000	0.04	A	Delacroix et al., 2024	4
Phytoplankton	~34-3400	3	B	Delacroix et al., 2024	5
Dissolved organic carbon	~270-6760	1	A	Santanelli et al., 2024	6
Phytoplankton	114-1171	~7	B	Faucher et al., 2025	7
Phytoplankton	10-100	~7	B	Hutchins et al., 2023	8
Plankton community	150-600	55	B	Ferderer et al., 2024	9
Corraline algae	760	21	B	Gore et al, 2019	10
Plankton community	500	21	B	Ferderer et al., 2022	11
Plankton community	361	21	B	Guo et al., 2024	12
Plankton community	511-2051	4	B	Subhas et al., 2022	13
Plankton community	300-2400	33	B	Marin-Samper et al., 2024	14
Plankton community	500	~20	B	Bach et al., 2024	15
Kelp	300-600	22	B	Britton et al., 2025	16
Phytoplankton	730-2740	4	B	Gately et al., 2023	17
Phytoplankton	100-1000	7-8	B	Oberlander et al., 2025	18
Phytoplankton	100-1000	0.04	A	Oberlander et al., 2025	19
Copepod	250-1250	4	B	Bhaumik et al., 2025	20
Plankton community	16-29	2	B	Guo et al., 2025	21
Benthic organisms	212-1246	4	B	Jones et al., 2025	22
Precipitation	250-1050	47	B	Moras et al., 2022	23
Precipitation	500-2000	0.007-47	A	Moras et al., 2022	24
Precipitation	300-2400	4	B	Hartmann et al., 2023	25
Precipitation	350-630	16-25	B	Moras et al., 2024	26
Precipitation	200-9200	20-25	B	Suitner et al. 2024	27
Precipitation/gas exchange	375-3305	68	B	Ringham et al., 2024	28
Precipitation/gas exchange	187-3829	15-40	B	Ringham et al., 2024	29

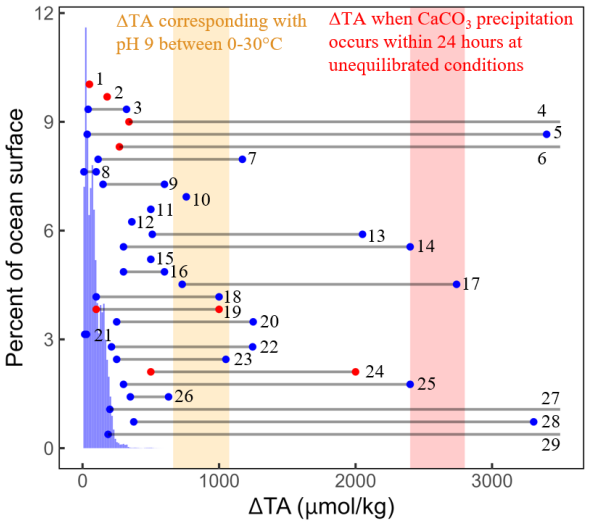

Exp	Comment
1	Interpreted as ocean acidification experiment but OAE has been mentioned.
4	Estimated by reported additions of 100g/L $Mg(OH)_2$ or 127 g/L $Ca(OH)_2$.
4,6	Upper end not shown in figure as ΔTA was >>3500 µmol/kg.
5	Estimated by reported additions of 1-100mg/L $Mg(OH)_2$.
6	Estimated by reported additions of 0.01-0.25g/L $Ca(OH)_2$.
8	Studied olivine but used a synthetic (fast dissolving) cocktail.
9,14	One of several papers from the same experiment.
15	Recommended ΔTA for currently 18 microcosm experiments.

4.2. Alkalinity perturbations from moving ships

A fast-dissolving alkalising agent added to the wake of a moving ship increased ΔTA to ~750-1500 µmol kg^{-1} (Fig. 2). This initial ΔTA would roughly elevate pH_T to ~9 under open ocean conditions, consistent with the regulatory threshold assumed herein (section 2.3.). ΔTA declines exponentially thereafter to ~2 (Chou 1996) and ~15 µmol kg^{-1} (IMCO 1975) one hour after ship passage. The IMCO equation is assumed to underestimate dilution and can therefore be seen as an upper bound (Chou 1996).

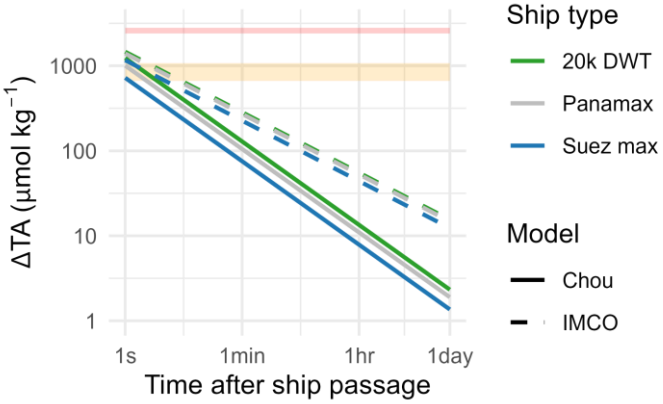

Figure 2. *Dilution of ΔTA in the wake of a ship. As in Table 1, the orange and red bands indicate potentially relevant regulatory thresholds for pH (orange) and geochemical thresholds for secondary carbonate precipitation (red).*

4.3. Alkalinity perturbations observed in the regional model

Regional OAE simulations considered two different TA delivery methods: 1) point sources of fully dissolved TA mimicking delivery of a fast-dissolving alkalising agent through three coastal outfalls, and 2) release from a slow-dissolving alkalising agent over a larger area of the seafloor (Fig. 3).

The point-source addition at a continuous rate of 12.5 mol s^{-1} from the Tufts Cove outfall (into the tidally mixed channel that connects the deep basin in Halifax Harbour to the open ocean) elevated TA by up to ~300 μmol L^{-1} near the release site (Fig. 3; please note that the regional model gives TA in a volume (μmol L^{-1}) but that this number is generally less than 3% different to the TA normalized to mass (μmol kg^{-1}) used elsewhere in the text). The maximum perturbation is larger in the simulation from July to September (~300 μmol L^{-1}), when the water column is thermally stratified. In the October to December simulation, when vertical mixing is larger than in summer, the maximum ΔTA is smaller at ~50 μmol L^{-1}. In both seasons, ΔTA of more than 10 μmol L^{-1}, which could be considered as an optimistic limit of detection given natural variability, occurs throughout the Harbour (see red isolines in Fig. 3). In the seafloor release simulation, after 2.5 years of continuous release, the ΔTA maxima are 8 μmol L^{-1} at the surface and 50 μmol L^{-1} at the bottom.

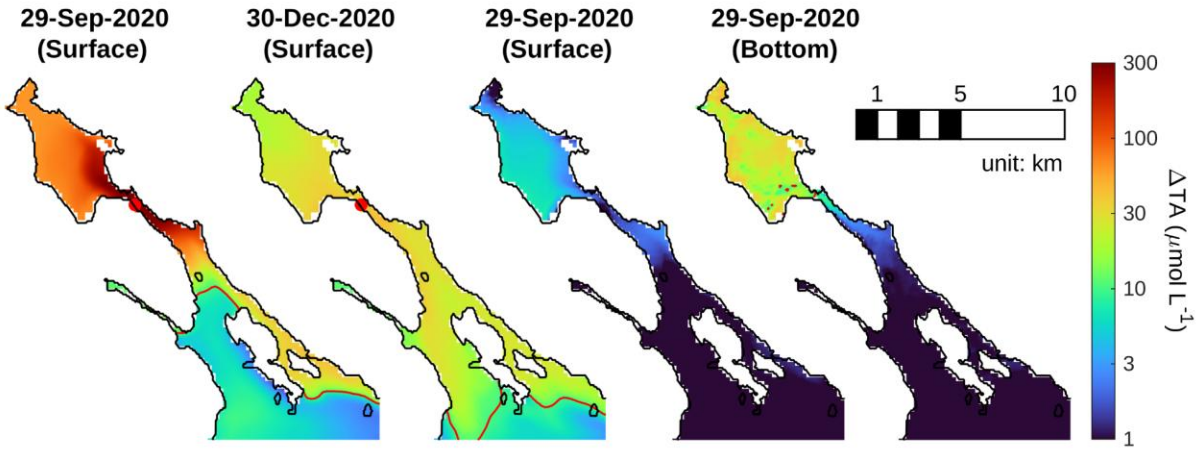

407

408 ***Figure 3****. Left two panels) Surface ΔTA simulated in Halifax Harbour after 3 months of*
409 *continuous TA addition from a point-source starting on July 1 and October 1, 2020. The*
410 *addition rate is 12.5 mol* s^{-1} *and occurs from the outfall at Tufts Cove (red dot). July-*
411 *September and October-December are the quarters resulting in the lowest and highest ΔTA*
412 *maxima. Right two panels) Surface and bottom ΔTA after 2.5 years of continuous release*
413 *from the sediments. The release rate is 1 mol* s^{-1} *throughout the entire Bedford Basin, i.e.*
414 *0.057 mol* km^{-2} s^{-1}*. Red isolines indicate ΔTA of 10* μmol L^{-1}.

415

416 The bathymetry and hydrography at the point source location have a large influence on the
417 transport and dispersion of ΔTA (Fig. 4). For release at Mill Cove at the head of the basin,
418 which is known to have a relatively long residence time of 55 to 65 days on average (Wang
419 *et al* 2025), average ΔTA reaches 300 μmol L^{-1}, similar to the maximum for the Tufts Cove
420 simulation, despite its much smaller addition rate of 3 mol s^{-1}. The elevated TA (>100 μmol L^{-1})
421 accumulates in the basin, an enclosed fjord-like system that is representative of other
422 enclosed bays, because of the restricted circulation. In contrast, at the Tufts Cove outfall,
423 which discharges into the tidally mixed channel, a similar maximum average ΔTA is reached
424 for an addition rate of 12.5 mol s^{-1} and there is less accumulation in the basin (Fig. 4). The
425 influence of the long residence time in the basin is visible in the bottom panels of Figure 4
426 after the discharge stops. For discharges from Mill Cove and Tufts Cove, more than 10^8 m^3 of

seawater are exposed to ΔTA of 10 μmol L^{-1} or more for at least a month after the addition stops.

For the point source release at Ketch Harbour, a small embayment adjacent to the open shelf, the ΔTA maximum is highly localized and decays within a few km from the outfall. In this case, ΔTA larger than 10 μmol L^{-1} extend only about 7 km in the alongshore direction and 3 km in the offshore direction (Fig. 4). The addition rate of 0.8 mol s^{-1} is the smallest of the three cases because it is dictated by the receiving grid cell in the small embayment. A more exposed location outside of the embayment would likely allow for a larger addition rate. However, the rapid decay of ΔTA within a shortest distance from the outfall would occur regardless of the exact placement of the outfall, because circulation in this region is not restricted by a semi-enclosed basin or channel. Once the addition stops, ΔTA dissipates entirely after just 15 days (Fig. 4).

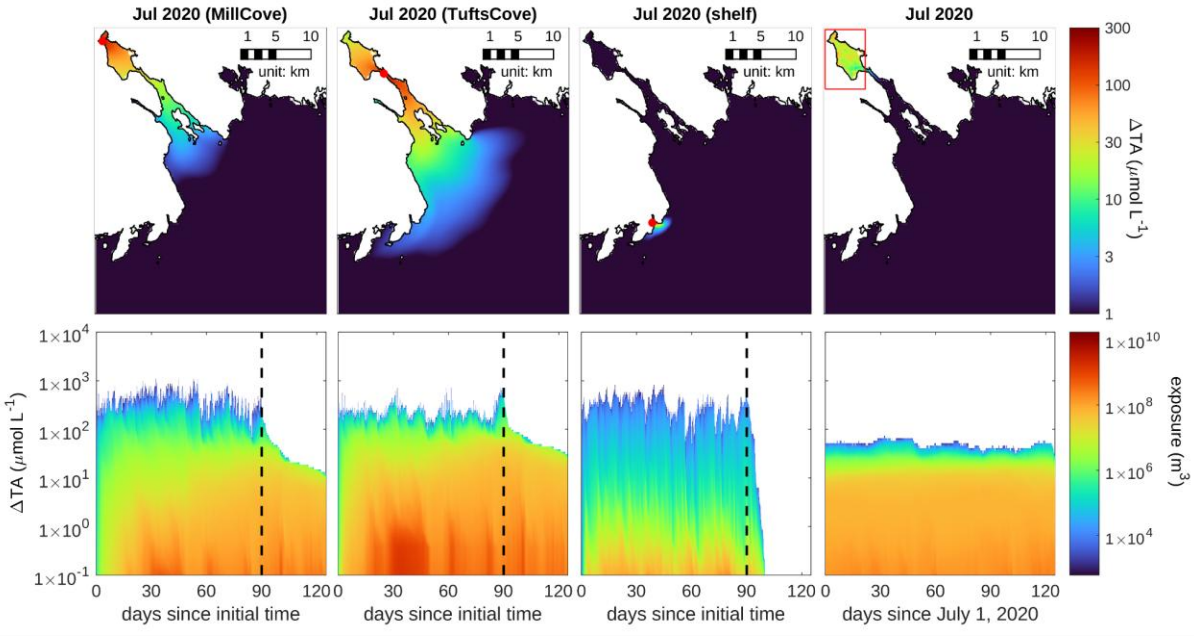

Figure 4*. Top panels) Average surface ΔTA over 3 months of continuous addition starting on July 1, 2020 from outfalls at Mill Cove (left), Tufts Cove (middle left), Ketch Harbour on the shelf (middle right), and evenly dispersed from the sediment in Bedford Basin (right). The sediment release simulation shows average ΔTA for the last 3 months of a 2-year continuous*

addition. Bottom panels) Volume of seawater (in colour) that is exposed to a range of ∆TA (y-axis) as the system evolves over time (x-axis) is shown corresponding to the panels above. Four months are shown where, for the point-source runs, the first three months see continuous TA addition followed by one month without any addition. The vertical dashed lines indicate when the addition stops.

In the simulation with slow sediment release, surface ΔTA in Bedford Basin ranges between 10 and 30 μmol L^{-1} and stays well below 100 μmol L^{-1} throughout the Basin. ΔTA rapidly decays to the unperturbed background value outside of the Basin (Fig. 4). Here again, the accumulation of ΔTA in Bedford Basin is the result of its restricted circulation and long residence time. After 2 years of continuous release a dynamical steady state is reached, where the slow addition of TA is balanced by advective and dispersive transport of ΔTA out of the basin. This is illustrated by the almost constant distribution of the exposure metric (in color) over the magnitude of ΔTA (y-axis) through time in Fig. 4 (bottom panel).

3.3. Alkalinity perturbations observed in a global model

Global ocean OAE simulations considered continuous TA additions in the coastal ocean of 335, 311, and 232 Tmol TA y^{-1} (determined in the 18th year of the simulation, after a steady-state rate was reached). Such TA release would eventually, after equilibration with the atmosphere, yield CDR on the order of approximately 12, 11, and 8 $GtCO_2$ yr^{-1} respectively.

The TA additions occurred homogeneously over large parts of the coastal surface ocean (within 100-150 km of the coast) and addition rate did not exceed ΔpH_T 0.1, hence never exceeding putative regulatory thresholds. After 18 years of globally dispersed OAE at the gigatonne-scale, ΔTA exceeds 200 μmol kg^{-1} in only 6%, 3.3%, and 0.33% of the ocean surface (0-100m), depending on the mode of dispersal (Fig. 5). Above 400 μmol kg^{-1}, these percentages decrease to 0.09%, 0.09% and 0.006%.

ΔTA remains generally much below 400 μmol kg^{-1} along coastlines where TA is added (Fig. 5). Regions with long coastlines (e.g. Java Sea or Caribbean) receive relatively higher TA inputs per ocean volume and therefore see generally higher ΔTA. Such higher input is also reflected in higher offshore ΔTA, like in the North-east Atlantic or Indian Ocean where ΔTA can reach up to around 300 μmol kg^{-1} after 18 years of simulation.

Marginal seas with limited exchange to the global ocean but more coastline relative to their seawater volume can have higher ΔTA (Fig. 5a). Here, we observe spatially averaged ΔTA of up to 250-750 μmol kg^{-1} (Baltic Sea), 200-300 μmol kg^{-1} (Mediterranean Sea), 200-350 μmol kg^{-1} (Persian Gulf), and 180-300 μmol kg^{-1} (Gulf of Mexico). However, because marginal seas have such limited exchange with the open ocean and small surface area for direct CO_2 gas exchange, the OAE deployment in such seas contributes very little to the overall TA addition globally. Thus, TA addition rates (and therefore ΔTA) could be significantly reduced without compromising the total OAE potential of the simulated scenario. It should also be noted that the global model used here may exhibit inferior accuracy for marginal seas compared to open sea areas - regional models should be preferred.

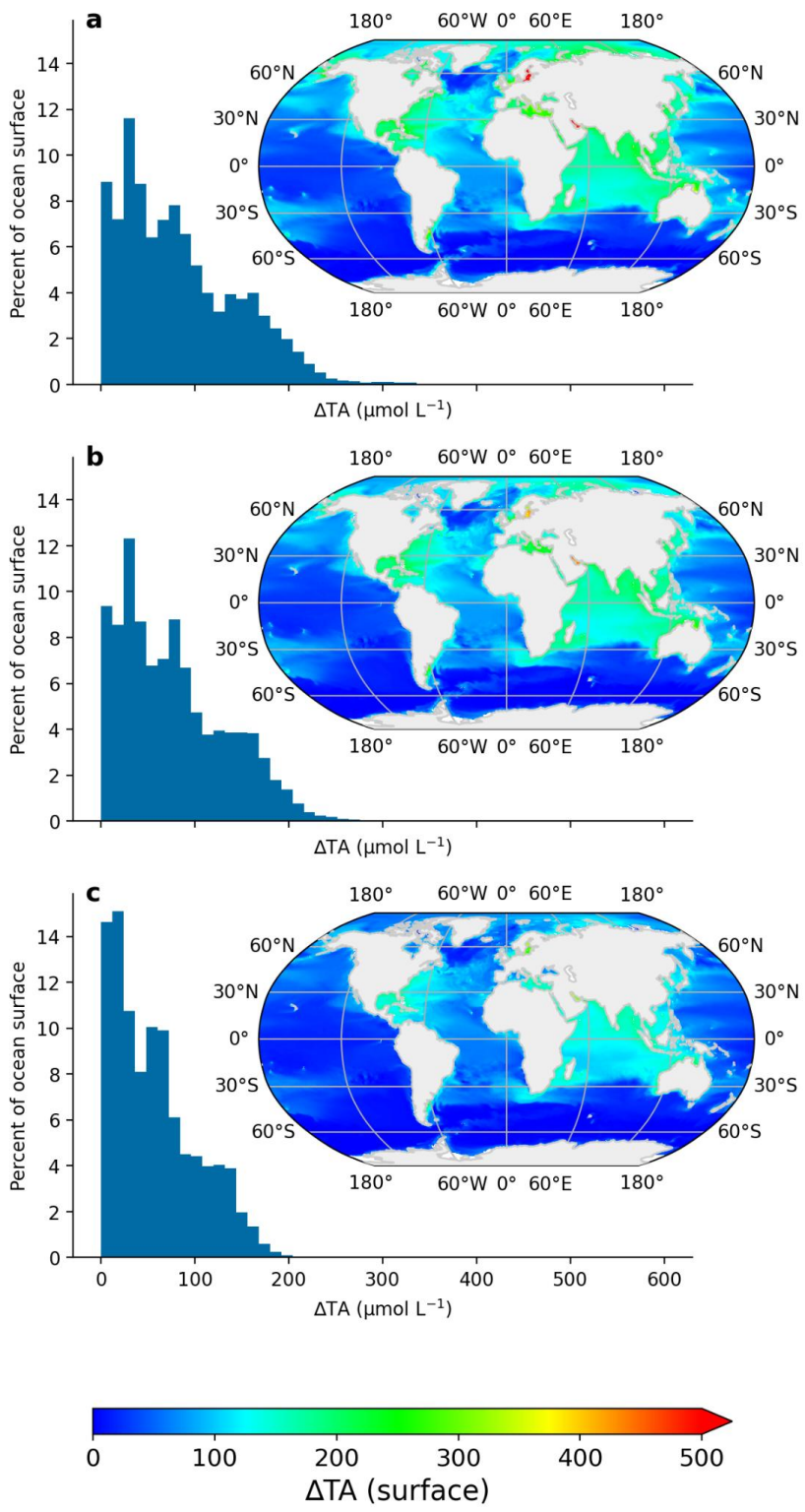

492

493 ***Figure 5***. *Maximal ΔTA (across the entire water column for each lat/long position) for*

494 *different continuous injection patterns after 18 years of simulation, shown as a map and as a*

495 *histogram. a) Injection in a continuous 111km coastal strip, CO_2 removal induced: 9GtCO_2 yr*

[1] b) Injection in coastal, 200km-separated spots, CO_2 removal induced: 11GtCO_2 yr^{-1} c) Injection in coastal, 400km-separated spots, negative emissions induced: 8.2GtCO_2 yr^{-1}.

5. Discussion

5.1. Plausible levels for alkalinity perturbations and implications for experimental design

Understanding both the rate and magnitude of OAE-induced changes to marine carbonate chemistry under realistic constraints is essential for informing the interpretation of OAE assessment studies. Table 2 synthesizes spatial and temporal scales and the assumed relevance of specific ΔTA ranges for specific scenarios. Importantly, a TA perturbation has larger potential to cause environmental effects before the invoked seawater CO_2 deficit has been equilibrated with atmospheric CO_2 due to larger pH and CO_2 amplitudes (Bach et al., 2019). The degree of equilibration, and thus the mitigation of impact potential, increases with time after perturbation over months to years (Zhou et al., 2025).

Exposure of organisms to ΔTA of >1000 µmol kg^{-1} could occur when a fast dissolving alkalising agent (e.g. NaOH, CaO) is discharged from a point source. Discharge from a moving vessel would invoke such ΔTA for seconds to minutes (Fig. 2) due to the ship wake which accelerates mixing and dilution (Chou 1996). Discharge and dilution from a coastal point source would not be supported by mechanical mixing, so that ΔTA of >1000 µmol kg^{-1} could theoretically be sustained for longer in systems with restricted circulation (high residence times). However, due to geochemical and regulatory constraints, coastal OAE point-sources would have to adjust the discharge rate according to natural dilution rates in the area of application to minimize the risk of TA loss through precipitation and stay within regulatory bounds. Thus, even coastal OAE point-sources would be unlikely to induce ΔTA of >1000 µmol kg^{-1} for much longer than minutes and only in a few m^3 where TA is added since

524 they are constrained by these external factors. Acute stress experiments, which expose
525 organisms to ∆TA >>1000 µmol kg^{-1} for several minutes to days (Table 1), should also
526 consider timescales below the minute as these may be most representative for OAE
527 methods using fast-dissolving or liquid alkalising agents in direct proximity to the release site.
528 Some may argue that ∆TA >1000 µmol kg^{-1} could occur after centuries of gigatonne-scale
529 OAE and its environmental implications are therefore relevant. However, in such a far future
530 scenario, OAE will long have been crucial for anthropogenic CO_2 management and hence
531 this hypothetical scenario would not be decisive on whether OAE should be upscaled in the
532 21st century. Environmental implications of such far future scenarios can arguably be
533 assessed more appropriately with natural analogue studies investigating high TA marginal
534 seas where such conditions already exist today (Table 2; Bach & Boyd, 2021).
535
536 ***Table 2.*** *Approximate spatial and temporal extents of simulated* ∆TA *and their derived*
537 *relevance for the environmental OAE assessment. The panel underneath underpins the*
538 *described spatio-temporal relevances of OAE-induced ∆TA with our model simulations.*
539 *Natural ∆TA was calculated as the difference of surface ocean (≲30 m depth) TA values*
540 *from the surface ocean mean TA (2305 µmol kg^{-1}; mean excludes marginal seas).*
541 *Climatological surface ocean TA data are originally from* Gregor and Gruber (2021) and
542 Mishonov *et al* (2023) *and were compiled for relevant basins* (Lehmann and Bach 2025).

ΔTA (μmol kg^{-1})	Timescale of the alkalinity perturbation	Spatial extent of the alkalinity perturbation	Relevance for the environmental OAE assessment
>1000	Seconds to minutes	Close to (within ~100s of meters) a fast-dissolving (e.g. NaOH) TA point source, such as a ship wake.	Relevant in extremely small and short-lived patches of seawater. Likely no relevance for OAE in the global ocean in the 21st century.
300-1000	Minutes to weeks in proximity to the release site. Years in enclosed basins under sustained gigatonne-scale deployment.	Near (within kilometers) of a point source or throughout enclosed basins under intense deployment along these coastlines.	Local relevance restricted to small patches of seawater under sustained and large deployments at point-sources. Globally relevant only in marginal seas with limited water exchange if intensively deployed therein for years.
100-300	Hours to years close to release sites. Longer-term relevance in ocean basins after years of gigatonne-scale deployment.	Downstream of local OAE sites. Occurs in ocean basins adjacent to abundant coastal OAE sites after years of gigatonne-scale deployment.	Locally relevant for large-scale deployments in coastal settings. Globally relevant downstream of OAE deployment hotspots after years of gigatonne-scale deployment.
1-100	Hours to years close to release sites. Years to millenia in the global ocean under gigatonne-scale deployment.	In the coastal ocean downstream of deployment sites. Majority of global ocean within this range after years of gigatonne-scale deployment.	Locally highly relevant for small and large-scale deployments. Globally relevant for much of the surface ocean.

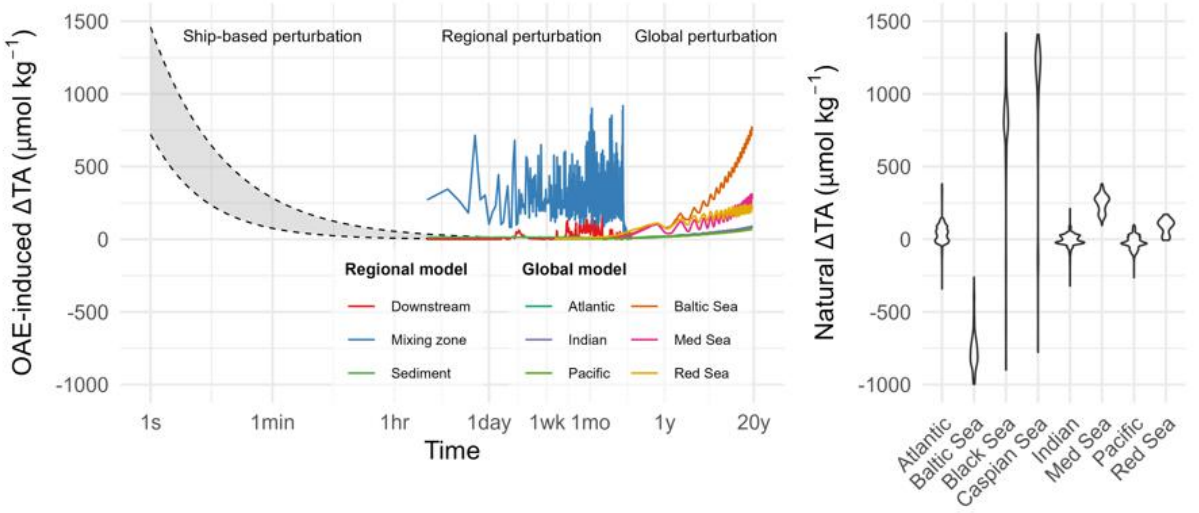

OAE within a ΔTA range of 300-1000 μmol kg^{-1} could be observable for minutes to weeks near TA point-sources. It could also be observed in semi-enclosed basins (e.g. Baltic Sea) where many large-scale OAE operations occur along the coastline for decades (Table 2). These levels could be locally/regionally important when water exchange with the bulk ocean

549 volume is limited. However, the ∆TA range of 300-1000 µmol kg^{-1} still has limited relevance
550 for global OAE deployments, even after decades of deployment at the gigatonne-scale (Fig.
551 5).
552
553 The ∆TA range <300 µmol kg^{-1} becomes increasingly widespread for OAE on a local and
554 global scale (Fig. 5) and is well within the range of natural surface ocean variability across
555 major ocean basins (Gregor and Gruber 2021). ∆TA from 100-300 µmol kg^{-1} can be found
556 downstream of OAE point sources (Fig. 4) and occurs in some major ocean basins (e.g.
557 Indian Ocean) after decades of gigatonne-scale OAE (Fig. 5). The range from 1-100 µmol kg^{-1}
558 is representative for even a larger volume downstream of local OAE deployment sites and
559 throughout the ocean (Table 2). This lowest ∆TA range considered here is by far the most
560 widespread for OAE in the 21st century.
561
562 **5.2. How marine organisms experience alkalinity perturbations**
563
564 To design and interpret environmental assessment studies it is important to elucidate how
565 marine organisms would experience OAE.
566
567 Plankton would experience OAE from a Lagrangian perspective - that is, they drift within an
568 OAE-perturbed seawater patch. In a point-source scenario, the patch gets gradually diluted
569 through mixing and diffusion with unperturbed (or less perturbed) seawater from the
570 surrounding. (Please note that other drivers of TA concentration changes such as rain and
571 evaporation are likely small compared to mixing and will be not further considered herein.)
572 Hence, the ∆TA would tend to decline over time, unless an already diluted patch of seawater
573 would mix with a patch containing a higher ∆TA. As such, plankton would generally
574 experience a sudden TA perturbation, which is most pronounced at the time when plankton
575 become entrained in the perturbed water mass for the first time. Based on the scenarios
576 simulated for Halifax Harbour, the highest ΔTA plankton could experience would be ~300

µmol kg^{-1} when entrained in a perturbed patch close to the point source (Figs. 3, 4). A TA perturbation, where TA is released slowly over a large area of the seafloor in Halifax Harbour, would induce moderately fluctuating ΔTA of <10 µmol kg^{-1} in the surface and mostly <40 µmol kg^{-1} near the bottom with some longer-term fluctuations due to bottom water flushing. The key difference to the point source scenario is the lower but more homogeneous discharge of TA over a larger area. As such, the perturbation amplitude is lower but the volume of similarly perturbed seawater is larger so that plankton would be exposed longer to more constant ΔTA (Fig. 4).

Benthic organisms experience OAE from a Eulerian perspective - that is, they are stationary with perturbed and unperturbed water masses passing by. In the point-source scenario, benthic communities reaching near the surface would be perturbed through fluctuating pulses of ΔTA (Fig. 6). However, fluctuations would be muted at depth due to dilution of the TA-perturbed seawater with unperturbed seawater before reaching the bottom layer. Here, OAE via a point-source would constitute a more homogeneous ΔTA (Fig. 6). Like for plankton, slow-release OAE from the sediment would expose benthos to less pronounced but more constant peaks in ΔTA.

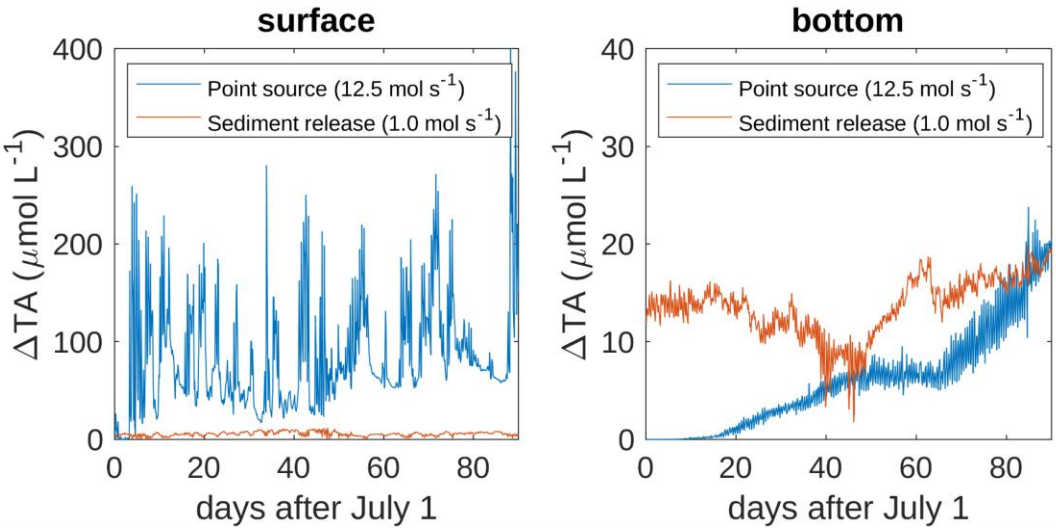

***Figure 6**. Local 3-month time series of ΔTA in 2020 resulting from a point source addition at*

the Tufts Cove outfall (blue) and the sediment-release simulation (red) at the surface (left) and bottom (right). The location is 10 grid points upstream from the Tufts Cove outfall in 46 m water depth.

Nekton, pelagic organisms that can swim against currents, are an interesting case in between that of plankton and benthos. They neither drift, nor are they stationary. If nektonic organisms can sense the TA perturbation they may actively avoid or migrate into it (Tigert and Porteus 2023). Otherwise they would randomly pass OAE-perturbed seawater patches, meaning they would be exposed to fluctuating ΔTA. Any projections on how nekton experience ΔTA are therefore difficult as there are two degrees of freedom: 1) Their migratory behaviour and 2) water mass movement. We note, however, that fish or whales in the open ocean migrate through latitudinal TA gradients of ~300 μmol kg^{-1}, similar in magnitude to imposed changes anticipated for OAE (Table 2). Furthermore, fish, dolphins and sharks migrate even more extreme gradients between marginal seas such as the Mediterranean and the Black Sea (Ulman *et al* 2020). As such, there is some evidence that nekton does not actively avoid high TA conditions.

The scenarios described for plankton, benthos and nekton consider immediate exposure to OAE from point sources. Organisms further away of point sources would experience TA perturbations after ΔTA from the various point sources would have mixed with the greater ocean volume and thus as an accumulation of ΔTA on the order of a few μmol kg^{-1} y^{-1} or less (e.g. in the open ocean Fig. 5). Hence, most marine organisms further away from point sources would experience OAE as a rather constant ΔTA, assuming that their lifetimes are between days up to a few years.

The above considerations underscore that OAE does not cause a homogeneous TA perturbation across the ocean ecosystem. Instead, ΔTA would be experienced heterogeneously, depending on organism lifestyles and their spatial and temporal proximity

to OAE sources. These factors should be taken into consideration when designing and interpreting experiments that investigate the effects of OAE on geochemical processes or environmental effects.

5.3. Adjusting the contextualization and communication of the experimental OAE assessment

The discussion thus far may suggest designing OAE experiments within the limits of plausible TA perturbations, thereby comparing biological responses observed under realistic ΔTA treatments with a control. A call for such "realistic scenario testing" is, however, not our intention. Instead of the experimental design, our argument addresses the contextualization and communication of OAE studies. This will be elaborated in the following.

Research into OAE, especially the environmental assessment, has to a large extent been moved forward by the ocean acidification (OA) research community (Oschlies *et al* 2023, Iglesias-Rodríguez *et al* 2023, Dupont and Metian 2023). Within the OA community, realistic scenario testing has initially been considered most useful to develop coherent recommendations for policymakers (Barry *et al* 2010). Indeed, abundant scenario testing enabled meta analyses (Kroeker *et al* 2013), which informed influential reports for policy (Bindoff *et al* 2019). However, scenario testing has later been criticized (1) to neglect the context-dependency of the outcome (i.e. different outcomes are possible in other environmental settings) and (2) to provide limited mechanistic understanding and thus value for modelling (Collins *et al* 2022, Paul and Bach 2020, Thomas and Ranjan 2024). Evolution of OA research into multiple stressor research gave room to reflect on the predominance and limitations of scenario testing (Boyd et al., 2018; Orr et al., 2020) and recently the OAE best practices guide recommended to expand the treatment range in OAE experiments into the extremes to gain mechanistic insights (i.e. ΔTA of 2000, 4000, 7000 μmol kg^{-1} (Iglesias-Rodríguez *et al* 2023)). Indeed, there are convincing arguments that "unrealistic

653 experiments" will increase chances to establish more reliable projections of organisms and
654 ecosystems under OAE through mechanistic understanding (Collins *et al* 2022).
655 Furthermore, experiments tackling the (unrealistic) extremes can be instrumental to unravel
656 processes that may be hard to detect but still relevant under "realistic" conditions. For
657 example, research with extremely high ∆TA was able to reveal potential geochemical
658 constraints on OAE through secondary precipitation (Moras *et al* 2022, 2024, Hartmann *et al*
659 2023, Ringham *et al* 2024, Suitner *et al* 2024) is also relevant for "more realistic" carbonate
660 chemistry conditions when seeds are abundant (Suitner *et al* 2025). It is possible that
661 progress on the matter would have been slower without the consideration of extreme
662 treatments.
663
664 The problem that could arise from the inclusion of extreme treatments for mechanistic
665 insights or detection of relevant processes is the following: In a study broadly contextualized
666 as OAE research, environmental effects observed at prolonged exposure to a ∆TA of, for
667 example, 2000, 4000, or 7000 µmol kg^{-1} would potentially be interpreted as an outcome
668 representative for OAE (if not by the author, quite likely by a non-expert reader). However,
669 such treatments are as representative for real-world OAE as pH 6 is representative for
670 anthropogenic ocean acidification - not representative at all. Thus, an OAE study that tests
671 environmental effects over prolonged periods at ∆TA of >1000 µmol kg^{-1} would have
672 assessed a relevant stressor (carbonate chemistry) but not the relevant stress level. Studies
673 that include such extreme ∆TA stress levels may need to carefully and explicitly flag these as
674 non-representative for OAE, or only representative for a very short time and very limited
675 spatial extent (Table 2). Such consideration is particularly important when coming up with a
676 title and abstract of an OAE study as these generally receive most attention in publications.
677 For example, a title that describes the outcome of a study may refrain from specifying OAE
678 as the driver of the response, if the described outcome occurred only at ∆TA levels beyond
679 what is plausible for OAE. Table 2 outlines the spatial and temporal scales over which ∆TA

680 simulated in experiments can be considered representative under real-world OAE
681 constraints.
682
683 **5. Conclusion**
684
685 Our study explored both how, and to what extent, OAE could perturb total alkalinity (TA), with
686 the aim of informing and ultimately improving environmental and geochemical assessments
687 of OAE. We acknowledge that some of the real-world constraints to OAE utilized herein
688 (section 2.) are based on assumptions which may change in the future. Hence, what is
689 deemed a "plausible level of OAE-induced ΔTA" herein may need to be reviewed in the
690 future.
691
692 On a local level, regulatory and geochemical constraints will likely set boundaries on how
693 much TA can be released per unit time into a water body. Both the regulatory and
694 geochemical limits could occur around pH 9, which is already a widespread legal threshold
695 for the release of wastewater (section 2.3.) and also in the approximate range where the risk
696 for TA loss via secondary precipitation is elevated, especially in the presence of seed
697 particles (section 2.4.). On a global level, OAE growth rate and the vast potential of the
698 ocean to dilute an TA perturbation (except for some marginal seas) will likely limit ΔTA to
699 <300 µmol kg^{-1}, even after years of gigatonne-scale CO_2 removal with OAE.
700
701 This study also elucidates how differently OAE will be perceived by the various marine
702 organisms and ecosystems. The heterogeneity of the OAE perturbation is even greater than
703 what was discussed herein for the many OAE pathways that not only perturb marine
704 carbonate chemistry but also introduce other chemicals such as trace metals or nutrients.
705 This suggests that experiments testing the effects of ΔTA on marine organisms or
706 ecosystems cannot easily be generalized as being representative for OAE in other contexts.
707 On the organism level, context-dependency can be addressed by designing experiments that

provide mechanistic understanding for an observed response (Collins *et al* 2022, Thomas and Ranjan 2024). Such experiments may require the inclusion of treatments that are not representative for TA perturbations anticipated for OAE in the real world (Ferderer *et al* 2025). To avoid potential bias by these treatments toward a stronger OAE response, it is important to contextualize the treatments as not directly representative for OAE.

Acknowledgements

LTB acknowledges funding from the Australian Research Council (grant no. FT200100846) and LTB and KF from the Carbon-to-Sea Initiative, a non-profit initiative dedicated to evaluating ocean alkalinity enhancement. KF and BW were also supported by the NSERC Alliance Missions grant ALLRP 570525-2021 and NSERC Discovery grant RGPIN-2022-02975.

Data Availability Statement

The ROMS model code is freely available at https://zenodo.org/records/14708820. The ROMS model output is freely available at https://zenodo.org/uploads/15347620. The simulation setup, code, and data files to simulate the surface alkalinity with ECCO and MITgcm can be found at https://zenodo.org/records/7474745

Author contributions

LTB, MDT, KF designed the study. BW, KF provided regional model results. MDT provided global model results. LTB drafted the manuscript. All authors revised and improved the draft.

Conflict of interest

736 The authors declare no conflict of interest.

737

738 **References**

739

740 https://www.imo.org/en/mediacentre/meetingsummaries/pages/lc-45-lp-18.aspxAlbright R,
741 Caldeira L, Hosfelt J, Kwiatkowski L, Maclaren J K, Mason B M, Nebuchina Y,
742 Ninokawa A, Pongratz J, Ricke K L, Rivlin T, Schneider K, Sesboüé M, Shamberger
743 K, Silverman J, Wolfe K, Zhu K and Caldeira K 2016 Reversal of ocean acidification
744 enhances net coral reef calcification *Nature* **531** 362–5

745 NASEM 2022 *A Research Strategy for Ocean-based Carbon Dioxide Removal and*
746 *Sequestration* (Washington, D.C.: National Academies Press) Online:
747 https://www.nap.edu/catalog/26278

748 Archer D, Eby M, Brovkin V, Ridgwell A, Cao L, Mikolajewicz U, Caldeira K, Matsumoto K,
749 Munhoven G, Montenegro A and Tokos K 2009 Atmospheric Lifetime of Fossil Fuel
750 Carbon Dioxide *Annual Review of Earth and Planetary Sciences* **37** 117–34

751 Bach L T and Boyd P W 2021 Seeking natural analogs to fast-forward the assessment of
752 marine CO2 removal *Proceedings of the National Academy of Sciences* **118**
753 e2106147118

754 Bach L T, Ferderer A J, LaRoche J and Schulz K G 2024 Technical note: Ocean Alkalinity
755 Enhancement Pelagic Impact Intercomparison Project (OAEPIIP) *Biogeosciences* **21**
756 3665–76

757 Bach L T, Gill S J, Rickaby R E M, Gore S and Renforth P 2019 CO2 Removal With
758 Enhanced Weathering and Ocean Alkalinity Enhancement: Potential Risks and Co-
759 benefits for Marine Pelagic Ecosystems *Frontiers in Climate* **1** Online:
760 https://www.frontiersin.org/articles/10.3389/fclim.2019.00007

761 Barry J P, Tyrrell T, Hansson L, Plattner G-K and Gattuso J-P 2010 Atmospheric CO2
762 targets for ocean acidification perturbation experiments *Guide to best practices for*
763 *ocean acidification research and data reporting* (Luxembourg: Publications Offi ce of
764 the European Union) pp 53–66

765 Bhaumik A, Faucher G, Henning M, Meunier C L and Boersma M 2025 Prey dynamics as a
766 buffer: enhancing copepod resilience to ocean alkalinity enhancement *Environ. Res.*
767 *Lett.* **20** 024058

768 Bindoff N L, Cheung W W L, Kairo J G, Aristegui J, Guinder V A, Hallberg R, Hilmi N, Jiao N,
769 Karim M S, Levin L, O'Donoghue S, Purca Cuicapusa S R, Rinkevich B, Suga T,
770 Tagliabue A and Williamson P 2019 Changing Ocean, Marine Ecosystems, and
771 Dependent Communities. In: IPCC Special Report on the Ocean and Cryosphere in a
772 Changing Climate [H.-O. Pörtner, D.C. Roberts, V. Masson-Delmotte, P. Zhai, M.
773 Tignor, E. Poloczanska, K. Mintenbeck, A. Alegría, M. Nicolai, A. Okem, J. Petzold,
774 B. Rama, N.M. Weyer (eds.)]. Cambridge University Press, Cambridge, UK and New
775 York, NY, USA, pp. 447–587. https://doi.org/10.1017/9781009157964.007. *Special*
776 *Report on the Ocean and Cryosphere in a Changing Climate* (UK and New York, NY,
777 USA: Cambridge University Press) pp 447–587 Online:
778 https://doi.org/10.1017/9781009157964.007

779 Boyd P W, Collins S, Dupont S, Fabricius K, Gattuso J-P, Havenhand J, Hutchins D A,
780 Riebesell U, Rintoul M S, Vichi M, Biswas H, Ciotti A, Gao K, Gehlen M, Hurd C L,
781 Kurihara H, McGraw C M, Navarro J M, Nilsson G E, Passow U and Pörtner H-O
782 2018 Experimental strategies to assess the biological ramifications of multiple drivers
783 of global ocean change—A review *Global Change Biology* **24** 2239–61

784 Brent K, Burns W and McGee J 2018 *Governance of Marine Geoengineering* (Waterloo:
785 Centre for International Governance Innovation (CIGI)) Online:
786 https://www.zbw.eu/econis-archiv/handle/11159/3660

787 Britton D, Visch W and Bach L T 2025 Moderate ocean alkalinity enhancement likely to have
788 minimal effects on a habitat-forming kelp across multiple life stages *Limnology and*
789 *Oceanography* **70** 1283–95

790 Carroll D, Menemenlis D, Adkins J F, Bowman K W, Brix H, Dutkiewicz S, Fenty I, Gierach M
791 M, Hill C, Jahn O, Landschützer P, Lauderdale J M, Liu J, Manizza M, Naviaux J D,
792 Rödenbeck C, Schimel D S, Van der Stocken T and Zhang H 2020 The ECCO-
793 Darwin Data-Assimilative Global Ocean Biogeochemistry Model: Estimates of
794 Seasonal to Multidecadal Surface Ocean pCO2 and Air-Sea CO2 Flux *Journal of*
795 *Advances in Modeling Earth Systems* **12** e2019MS001888

796 Caserini S, Pagano D, Campo F, Abbà A, De Marco S, Righi D, Renforth P and Grosso M
797 2021 Potential of Maritime Transport for Ocean Liming and Atmospheric CO2
798 Removal *Front. Clim.* **3** Online:
799 https://www.frontiersin.org/journals/climate/articles/10.3389/fclim.2021.575900/full

800 Caserini S, Storni N and Grosso M 2022 The Availability of Limestone and Other Raw
801 Materials for Ocean Alkalinity Enhancement *Global Biogeochemical Cycles* **36**
802 e2021GB007246

803 Chou H-T 1996 On the dilution of liquid waste in ships' wakes *J Mar Sci Technol* **1** 149–54

804 Collins S, Whittaker H and Thomas M K 2022 The need for unrealistic experiments in global
805 change biology *Current Opinion in Microbiology* **68** 102151

806 Cripps G, Widdicombe S, Spicer J I and Findlay H S 2013 Biological impacts of enhanced
807 alkalinity in *Carcinus maenas Marine Pollution Bulletin* **71** 190–8

808 Delacroix S, Nystuen T J, Tobiesen A E D, King A L and Höglund E 2024 Ocean alkalinity
809 enhancement impacts: regrowth of marine microalgae in alkaline mineral
810 concentrations simulating the initial concentrations after ship-based dispersions
811 *Biogeosciences* **21** 3677–90

812 Donlon C, Robinson I, Casey K S, Vazquez-Cuervo J, Armstrong E, Arino O, Gentemann C,
813 May D, LeBorgne P, Piollé J, Barton I, Beggs H, Poulter D J S, Merchant C J,
814 Bingham A, Heinz S, Harris A, Wick G, Emery B, Minnett P, Evans R, Llewellyn-
815 Jones D, Mutlow C, Reynolds R W, Kawamura H and Rayner N 2007 The Global
816 Ocean Data Assimilation Experiment High-resolution Sea Surface Temperature Pilot
817 Project Online: https://journals.ametsoc.org/view/journals/bams/88/8/bams-88-8-
818 1197.xml

819 Duckham C 2013 *Impacts of ocean acidification and mitigative hydrated lime addition on*
820 *Pacific oyster larvae: implications for shellfish aquaculture* Master thesis (Burnaby,
821 Canada: Simon Fraser University) Online: https://summit.sfu.ca/item/13500

Dupont S and Metian M 2023 General considerations for experimental research on ocean alkalinity enhancement *State of the Planet* **2-oae2023** 1–11

Dutkiewicz S, Solkov A P, Scott J and Stone P H 2005 *A three-dimensional ocean-seaice-carbon cycle model and its coupling to a two-dimensional atmospheric model: Uses in climate change studies* Online: http://hdl. handle.net/1721.1/18091

Egbert G D and Erofeeva S Y 2002 Efficient Inverse Modeling of Barotropic Ocean Tides Online: https://journals.ametsoc.org/view/journals/atot/19/2/1520-0426_2002_019_0183_eimobo_2_0_co_2.xml

Eisaman M D 2024 Pathways for marine carbon dioxide removal using electrochemical acid-base generation *Front. Clim.* **6** Online: https://www.frontiersin.org/journals/climate/articles/10.3389/fclim.2024.1349604/full

Eisaman M D, Geilert S, Renforth P, Bastianini L, Campbell J, Dale A W, Foteinis S, Grasse P, Hawrot O, Löscher C R, Rau G H and Rønning J 2023 Assessing the technical aspects of ocean-alkalinity-enhancement approaches *State of the Planet* **2-oae2023** 1–29

England P I and Bach L T 2025 Influence of Wave Action on Applications of Olivine-Based Ocean Alkalinity Enhancement on Sandy Beaches *Geophysical Research Letters* **52** e2025GL114922

Ferderer A, Chase Z, Kennedy F, Schulz K G and Bach L T 2022 Assessing the influence of ocean alkalinity enhancement on a coastal phytoplankton community *Biogeosciences* **19** 5375–99

Ferderer A, Schulz K G, Riebesell U, Baker K G, Chase Z and Bach L T 2024 Investigating the effect of silicate- and calcium-based ocean alkalinity enhancement on diatom silicification *Biogeosciences* **21** 2777–94

Ferderer A, Schulz K G, Willis A, Baker K G, Chase Z and Bach L T 2025 Carbonate chemistry fitness landscapes inform diatom resilience to future perturbations *Science Advances* **11** eadu8024

Fuhr M, Dale A W, Wallmann K, Bährle R, Kalapurakkal H T, Sommer S, Spiegel T, Dobashi R, Buchholz B, Schmidt M, Perner M and Geilert S 2025 Calcite is an efficient and low-cost material to enhance benthic weathering in shelf sediments of the Baltic Sea *Commun Earth Environ* **6** 106

Fuhr M, Geilert S, Schmidt M, Liebetrau V, Vogt C, Ledwig B and Wallmann K 2022 Kinetics of Olivine Weathering in Seawater: An Experimental Study *Front. Clim.* **4** Online: https://www.frontiersin.org/journals/climate/articles/10.3389/fclim.2022.831587/full

Gately J A, Kim S M, Jin B, Brzezinski M A and Iglesias-Rodriguez M D 2023 Coccolithophores and diatoms resilient to ocean alkalinity enhancement: A glimpse of hope? *Science Advances* **9** eadg6066

Geerts L J J, Hylén A and Meysman F J R 2025 Review and syntheses: Ocean alkalinity enhancement and carbon dioxide removal through marine enhanced rock weathering using olivine *Biogeosciences* **22** 355–84

Gentile E, Tarantola F, Lockley A, Vivian C and Caserini S 2022 Use of aircraft in ocean alkalinity enhancement *Science of The Total Environment* **822** 153484

Gidden M J, Roe S, Ganti G, Gasser T, Hasegawa T, Lamb W F, Ochi Y, Strefler J and Vaughan N E 2024 Paris-consistent CDR scenarios *The State of Carbon Dioxide Removal 2024 – 2nd Edition* Online: https://www.stateofcdr.org

Gore S, Renforth P and Perkins R 2019 The potential environmental response to increasing oceanalkalinity for negative emissions *Mitig Adapt Strateg Glob Change* **24** 1191–211

Graham E, Fulghum N and Altieri K 2025 *Global Electricity Review 2025* Online: https://ember-energy.org/app/uploads/2025/04/Report-Global-Electricity-Review-2025.pdf

Gregor L and Gruber N 2021 OceanSODA-ETHZ: a global gridded data set of the surface ocean carbonate system for seasonal to decadal studies of ocean acidification *Earth System Science Data* **13** 777–808

Guo J A, Strzepek R F, Swadling K M, Townsend A T and Bach L T 2024 Influence of ocean alkalinity enhancement with olivine or steel slag on a coastal plankton community in Tasmania *Biogeosciences* **21** 2335–54

Guo J A, Strzepek R F, Yuan Z, Swadling K M, Townsend A T, Achterberg E P, Browning T J and Bach L T 2025 Effects of ocean alkalinity enhancement on plankton in the Equatorial Pacific *Commun Earth Environ* **6** 270

Haidvogel D B, Arango H, Budgell W P, Cornuelle B D, Curchitser E, Di Lorenzo E, Fennel K, Geyer W R, Hermann A J, Lanerolle L, Levin J, McWilliams J C, Miller A J, Moore A M, Powell T M, Shchepetkin A F, Sherwood C R, Signell R P, Warner J C and Wilkin J 2008 Ocean forecasting in terrain-following coordinates: Formulation and skill assessment of the Regional Ocean Modeling System *Journal of Computational Physics* **227** 3595–624

Halifax Water 2025 Publications & Reports | Halifax Water Online: https://halifaxwater.ca/publications-reports

Hartmann J, Suitner N, Lim C, Schneider J, Marín-Samper L, Arístegui J, Renforth P, Taucher J and Riebesell U 2023 Stability of alkalinity in ocean alkalinity enhancement (OAE) approaches – consequences for durability of CO_2 storage *Biogeosciences* **20** 781–802

Hartmann J, West A J, Renforth P, Köhler P, De La Rocha C L, Wolf-Gladrow D A, Dürr H H and Scheffran J 2013 Enhanced chemical weathering as a geoengineering strategy to reduce atmospheric carbon dioxide, supply nutrients, and mitigate ocean acidification *Reviews of Geophysics* **51** 113–49

He J and Tyka M D 2023 Limits and CO_2 equilibration of near-coast alkalinity enhancement *Biogeosciences* **20** 27–43

Hersbach H, Bell B, Berrisford P, Hirahara S, Horányi A, Muñoz-Sabater J, Nicolas J, Peubey C, Radu R, Schepers D, Simmons A, Soci C, Abdalla S, Abellan X, Balsamo G, Bechtold P, Biavati G, Bidlot J, Bonavita M, De Chiara G, Dahlgren P, Dee D, Diamantakis M, Dragani R, Flemming J, Forbes R, Fuentes M, Geer A, Haimberger L, Healy S, Hogan R J, Hólm E, Janisková M, Keeley S, Laloyaux P, Lopez P, Lupu C, Radnoti G, de Rosnay P, Rozum I, Vamborg F, Villaume S and Thépaut J-N 2020 The ERA5 global reanalysis *Quarterly Journal of the Royal Meteorological Society* **146** 1999–2049

House K Z, House C H, Schrag D P and Aziz M J 2007 Electrochemical Acceleration of Chemical Weathering as an Energetically Feasible Approach to Mitigating Anthropogenic Climate Change *Environ. Sci. Technol.* **41** 8464–70

Iglesias-Rodríguez M D, Rickaby R E M, Singh A and Gately J A 2023 Laboratory experiments in ocean alkalinity enhancement research *State of the Planet* **2-oae2023** 1–18

IMCO 1975 *Procedures and arrangements for the discharge of noxious liquid substances. Method for calculation of dilution capacity in the ship's wake*

IMO 2023 45th Consultative Meeting of Contracting Parties to the London Convention and the 18th Meeting of Contracting Parties to the London Protocol (LC 45/LP 18) Online: https://www.imo.org/en/mediacentre/meetingsummaries/pages/lc-45-lp-18.aspx

Jean-Michel L, Eric G, Romain B-B, Gilles G, Angélique M, Marie D, Clément B, Mathieu H, Olivier L G, Charly R, Tony C, Charles-Emmanuel T, Florent G, Giovanni R, Mounir B, Yann D and Pierre-Yves L T 2021 The Copernicus Global 1/12° Oceanic and Sea Ice GLORYS12 Reanalysis *Front. Earth Sci.* **9** Online: https://www.frontiersin.org/journals/earth-science/articles/10.3389/feart.2021.698876/full

Jones K, Hemery L G, Ward N D, Regier P J, Ringham M C and Eisaman M D 2025 Biological response of eelgrass epifauna, Taylor's Sea hare (*Phyllaplysia taylori*) and eelgrass isopod (*Idotea resecata*), to elevated ocean alkalinity *Biogeosciences* **22** 1615–30

Khangaonkar T, Carter B R, Premathilake L, Yun S K, Ni W, Stoll M M, Ward N D, Hemery L G, Torres Sanchez C, Subban C V, Ringham M C, Eisaman M D, Pelman T, Tallam K and Feely R A 2024 Mixing and dilution controls on marine CO2 removal using alkalinity enhancement *Environ. Res. Lett.* **19** 104039

Kheshgi H S 1995 Sequestering atmospheric carbon dioxide by increasing ocean alkalinity *Energy* **20** 915–22

Köhler P, Abrams J F, Völker C, Hauck J and Wolf-Gladrow D A 2013 Geoengineering impact of open ocean dissolution of olivine on atmospheric CO2, surface ocean pH and marine biology *Environ. Res. Lett.* **8** 014009

Kroeker K J, Kordas R L, Crim R, Hendriks I E, Ramajo L, Singh G S, Duarte C M and Gattuso J-P 2013 Impacts of ocean acidification on marine organisms: quantifying sensitivities and interaction with warming *Global Change Biology* **19** 1884–96

Lauvset S K, Key R M, Olsen A, van Heuven S, Velo A, Lin X, Schirnick C, Kozyr A, Tanhua T, Hoppema M, Jutterström S, Steinfeldt R, Jeansson E, Ishii M, Perez F F, Suzuki T and Watelet S 2016 A new global interior ocean mapped climatology: the 1° × 1° GLODAP version 2 *Earth System Science Data* **8** 325–40

Lehmann N and Bach L T 2025 Global carbonate chemistry gradients reveal a negative feedback on ocean alkalinity enhancement *Nat. Geosci.* **18** 232–8

Marín-Samper L, Arístegui J, Hernández-Hernández N and Riebesell U 2024 Responses of microbial metabolic rates to non-equilibrated silicate- versus calcium-based ocean alkalinity enhancement *Biogeosciences* **21** 5707–24

Mishonov A V, Boyer T P, Baranova O K, Bouchard C N, Cross S L, Garcia H E, Locarnini R A, Paver C R, Reagan J R, Wang Z, Seidov D, Grodsky A I and Beauchamp J G 2023 *World Ocean Database 2023* (National Oceanographic and Atmospheric Administration) Online: https://repository.library.noaa.gov/view/noaa/66204

Moras C A, Bach L T, Cyronak T, Joannes-Boyau R and Schulz K G 2022 Ocean alkalinity enhancement – avoiding runaway $CaCO_3$ precipitation during quick and hydrated lime dissolution *Biogeosciences* **19** 3537–57

Moras C A, Cyronak T, Bach L T, Joannes-Boyau R and Schulz K G 2024 Effects of grain size and seawater salinity on magnesium hydroxide dissolution and secondary calcium carbonate precipitation kinetics: implications for ocean alkalinity enhancement *Biogeosciences* **21** 3463–75

Morse J W, Arvidson R S and Lüttge A 2007 Calcium Carbonate Formation and Dissolution *Chem. Rev.* **107** 342–81

Moum J N 2021 Variations in Ocean Mixing from Seconds to Years *Annual Review of Marine Science* **13** 201–26

Mu L, Palter J B and Wang H 2023 Considerations for hypothetical carbon dioxide removal via alkalinity addition in the Amazon River watershed *Biogeosciences* **20** 1963–77

Oberlander J L, Burke M E, London C A and MacIntyre H L 2025 Assessing the impacts of simulated ocean alkalinity enhancement on viability and growth of nearshore species of phytoplankton *Biogeosciences* **22** 499–512

Orr J A, Vinebrooke R D, Jackson M C, Kroeker K J, Kordas R L, Mantyka-Pringle C, Van den Brink P J, De Laender F, Stoks R, Holmstrup M, Matthaei C D, Monk W A, Penk M R, Leuzinger S, Schäfer R B and Piggott J J 2020 Towards a unified study of multiple stressors: divisions and common goals across research disciplines *Proceedings of the Royal Society B: Biological Sciences* **287** 20200421

Oschlies A, Bach L T, Rickaby R E M, Satterfield T, Webb R and Gattuso J-P 2023 Climate targets, carbon dioxide removal, and the potential role of ocean alkalinity enhancement *State of the Planet* **2-oae2023** 1–9

Paul A J and Bach L T 2020 Universal response pattern of phytoplankton growth rates to increasing CO2 *New Phytologist* **228** 1710–6

Paul A J, Haunost M, Goldenberg S U, Hartmann J, Sánchez N, Schneider J, Suitner N and Riebesell U 2024 Ocean alkalinity enhancement in an open ocean ecosystem: Biogeochemical responses and carbon storage durability *EGUsphere* 1–31

Penman D E, Caves Rugenstein J K, Ibarra D E and Winnick M J 2020 Silicate weathering as a feedback and forcing in Earth's climate and carbon cycle *Earth-Science Reviews* **209** 103298

Renforth P and Henderson G 2017 Assessing ocean alkalinity for carbon sequestration *Reviews of Geophysics* **55** 636–74

Ringham M C, Hirtle N, Shaw C, Lu X, Herndon J, Carter B R and Eisaman M D 2024 An assessment of ocean alkalinity enhancement using aqueous hydroxides: kinetics, efficiency, and precipitation thresholds *Biogeosciences* **21** 3551–70

990 Santinelli C, Valsecchi S, Retelletti Brogi S, Bachi G, Checcucci G, Guerrazzi M, Camatti E,
991 Caserini S, Azzellino A and Basso D 2024 Ocean liming effects on dissolved organic
992 matter dynamics *Biogeosciences* **21** 5131–41

993 Savoie A M, Ringham M, Torres Sanchez C, Carter B R, Dougherty S, Feely R A, Hegeman
994 D, Herndon J, Khangaonkar T, Loretz J, Minck T, Pelman T, Premathilake L, Subban
995 C, Vance J and Ward N D 2025 Novel field trial for ocean alkalinity enhancement
996 using electrochemically derived aqueous alkalinity *Front. Environ. Eng.* **4** Online:
997 https://www.frontiersin.org/journals/environmental-
998 engineering/articles/10.3389/fenve.2025.1641277/full

999 Shan S, Sheng J, Thompson K R and Greenberg D A 2011 Simulating the three-dimensional
1000 circulation and hydrography of Halifax Harbour using a multi-nested coastal ocean
1001 circulation model *Ocean Dynamics* **61** 951–76

1002 Smith S M, Geden O, Gidden M J, Lamb W F, Nemet G, Minx J C, Buck H, Burke J, Cox E,
1003 Edwards M R, Fuss S, Johnstone I, Muller-Hansen F, Pongartz J, Probst B S, Roe S,
1004 Schenuit F, Schulte I and Vaughan N E 2024 *The State of Carbon Dioxide Removal*
1005 *2024 - 2nd Edition* Online: https://www.stateofcdr.org

1006 Subhas A V, Marx L, Reynolds S, Flohr A, Mawji E W, Brown P J and Cael B B 2022
1007 Microbial ecosystem responses to alkalinity enhancement in the North Atlantic
1008 Subtropical Gyre *Front. Clim.* **4** Online:
1009 https://www.frontiersin.org/journals/climate/articles/10.3389/fclim.2022.784997/full

1010 Suitner N, Faucher G, Lim C, Schneider J, Moras C A, Riebesell U and Hartmann J 2024
1011 Ocean alkalinity enhancement approaches and the predictability of runaway
1012 precipitation processes: results of an experimental study to determine critical
1013 alkalinity ranges for safe and sustainable application scenarios *Biogeosciences* **21**
1014 4587–604

1015 Suitner N, Hartmann J, Varliero S, Faucher G, Suessle P and Moras C A 2025 Surface area
1016 and Ω-aragonite oversaturation as controls of the runaway precipitation
1017 process in ocean alkalinity enhancement *EGUsphere* 1–26

1018 Tchobanoglous G, Stensel H, Tsuchihashi R and Burton F 2013 *Wastewater Engineering:*
1019 *Treatment and Resource Recovery* (McGraw-Hill)

1020 Thomas M K and Ranjan R 2024 Designing More Informative Multiple-Driver Experiments
1021 *Annual Review of Marine Science* **16** 513–36

1022 Tigert L R and Porteus C S 2023 Invited review - the effects of anthropogenic abiotic
1023 stressors on the sensory systems of fishes *Comparative Biochemistry and Physiology*
1024 *Part A: Molecular & Integrative Physiology* **277** 111366

1025 Ulman A, Zengin M, Demirel N and Pauly D 2020 The Lost Fish of Turkey: A Recent History
1026 of Disappeared Species and Commercial Fishery Extinctions for the Turkish Marmara
1027 and Black Seas *Front. Mar. Sci.* **7** Online: https://www.frontiersin.org/journals/marine-
1028 science/articles/10.3389/fmars.2020.00650/full

1029 Wang B, Laurent A, Pei Q, Sheng J, Atamanchuk D and Fennel K 2025 Maximizing the
1030 Detectability of Ocean Alkalinity Enhancement (OAE) While Minimizing Its Exposure
1031 Risks: Insights From a Numerical Study *Earth's Future* **13** e2024EF005463

1032 Wang H, Pilcher D J, Kearney K A, Cross J N, Shugart O M, Eisaman M D and Carter B R

2023 Simulated Impact of Ocean Alkalinity Enhancement on Atmospheric CO2 Removal in the Bering Sea *Earth's Future* **11** e2022EF002816

Wanninkhof R 1992 Relationship between wind speed and gas exchange over the ocean *Journal of Geophysical Research: Oceans* **97** 7373–82

Wateroffice Canada 2025 Real-Time Hydrometric Data Graph for SACKVILLE RIVER AT BEDFORD (01EJ001) [NS] - Water Level and Flow - Environment Canada Online: https://wateroffice.ec.gc.ca/report/real_time_e.html?stn=01EJ001

Wurgaft E, Wang Z A, Churchill J H, Dellapenna T, Song S, Du J, Ringham M C, Rivlin T and Lazar B 2021 Particle Triggered Reactions as an Important Mechanism of Alkalinity and Inorganic Carbon Removal in River Plumes *Geophysical Research Letters* **48** e2021GL093178

Zhang H, Menemenlis D and Fenty I 2018 ECCO LLC270 Ocean-Ice State Estimate Online: https://dspace.mit.edu/handle/1721.1/119821

Zhong S and Mucci A 1989 Calcite and aragonite precipitation from seawater solutions of various salinities: Precipitation rates and overgrowth compositions *Chemical Geology* **78** 283–99

Zhou M, Tyka M D, Ho D T, Yankovsky E, Bachman S, Nicholas T, Karspeck A R and Long M C 2025 Mapping the global variation in the efficiency of ocean alkalinity enhancement for carbon dioxide removal *Nat. Clim. Chang.* **15** 59–65

Supplementary material

Table S1. upper pH thresholds of various countries for wastewater release.

Country	pH	Reference
Namibia	9.5	https://faolex.fao.org/docs/pdf/nam224871.pdf
South Africa	9.5	https://faolex.fao.org/docs/pdf/saf194025.pdf
Samoa	9.5	https://faolex.fao.org/docs/pdf/sam150409.pdf
Cambodia	9	https://faolex.fao.org/docs/pdf/cam47646.pdf
China	9	https://chinawaterrisk.org/wp-content/uploads/2011/05/Maximum-Allowable-Discharge-Concentrations-For-Other-Pollutants-in-China.pdf
Ecuador	9	https://www.frontiersin.org/journals/environmental-science/articles/10.3389/fenvs.2020.00030/full
Germany	9	https://faolex.fao.org/docs/pdf/ger89269.pdf
India	9	https://www.frontiersin.org/journals/environmental-science/articles/10.3389/fenvs.2020.00030/full
Kenya	9	https://faolex.fao.org/docs/pdf/ken84962.pdf
Malaysia	9	https://faolex.fao.org/docs/pdf/mal102817.pdf
Mauritius	9	https://faolex.fao.org/docs/pdf/mat52519.pdf
Saudi Arabia	9	https://faolex.fao.org/docs/pdf/sau213688.pdf
Papua New Guinea	9	https://faolex.fao.org/docs/pdf/png202942.pdf
France	8.5	https://www.frontiersin.org/journals/environmental-science/articles/10.3389/fenvs.2020.00030/full
Nigeria	8.5	https://faolex.fao.org/docs/pdf/nig204466.pdf
Sri Lanka	8.5	https://faolex.fao.org/docs/pdf/SRL224512.pdf
Tanzania	8.5	https://www.frontiersin.org/journals/environmental-science/articles/10.3389/fenvs.2020.00030/full
Uganda	8.5	https://faolex.fao.org/docs/pdf/uga203300.pdf

Figure S1.

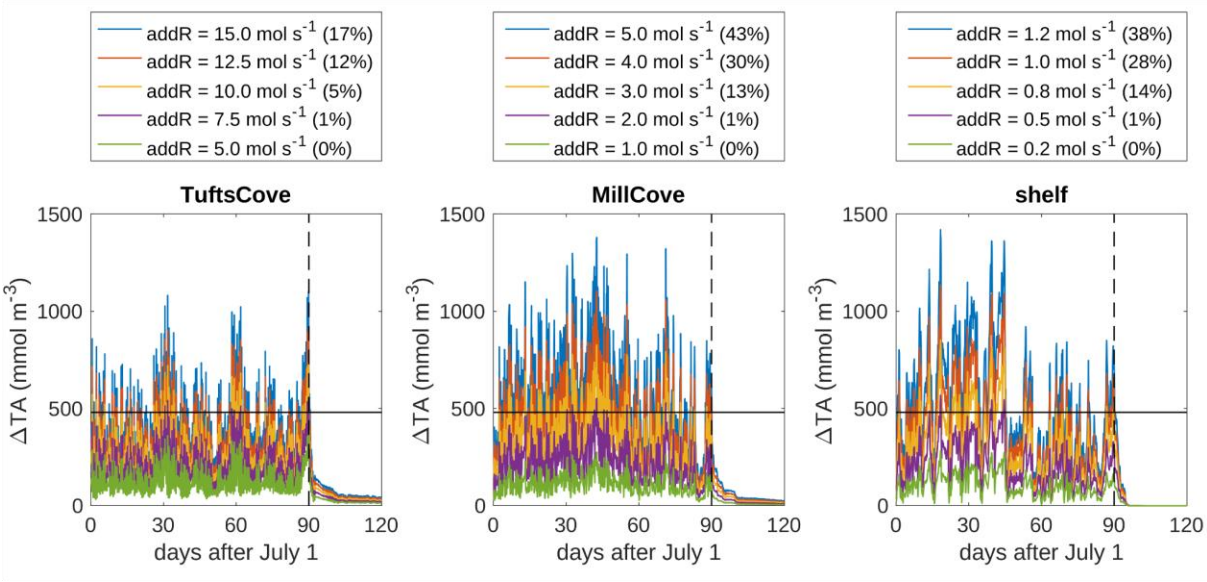

1060

1061

1062 **Figure S1**. Evolution of ΔTA in the grid cells receiving the alkalinity addition for three
1063 simulated coastal outfalls and a range of constant addition rates (addR; see legends
1064 corresponding to each of the three panels). The number in parentheses after each addition
1065 rate indicates the percentage of time during ongoing addition where ΔTA exceeds 480 mmol
1066 m^{-3} (indicated by the black line and corresponding to pH of 9 in this setting). The vertical
1067 dashed lines indicate when the addition was stopped.